marker motion during an arc with irregular breathing. Intrafraction motion caused a mean 3D target position error of 3.3 mm, resulting in a mean D_{95} reduction of 6.6% over all fractions. The D_{95} reduction correlated with the mean 3D target position error during a fraction ($p < 0.001$, Fig. B).
Conclusions: Kilovoltage imaging for detailed motion monitoring and dose reconstruction during VMAT liver SBRT was demonstrated for the first time. Large dosimetric impact of intrafraction tumor motion was observed. Although all patients received the prescribed dose (since dose is prescribed to the 67% level) the results show that intrafraction motion adaptation is warranted to maximize the CTV dose, especially for SBRT treatments where the convention has been to prescribe a peaked non-uniform PTV dose that gradually decreases outside the CTV.

OC-0333
Accurate tumor tracking requires a 4D CT scan to select markers moving synchrone to the tumor
N.C.M.G. van der Voort van Zyp[1], J.J. Nuyttens[1], M.S. Hoogeman[1]
[1]*Erasmus Medical Center Rotterdam, Radiation Oncology, Rotterdam, The Netherlands*

Purpose/Objective: Markers are often used to track lung tumors. However markers placed outside the tumor may not move synchronously to the tumor during breathing thereby potentially introducing errors in tumor tracking. The purpose of this study is to identify factors which influence non-synchronous marker motion, and to evaluate methods to exclude markers for tumor tracking in order to minimize the tracking error.
Materials and Methods: Data of 53 patients with 64 tumors were studied. Marker and tumor motion was assessed using a 4DCT scan. In-house developed software was used to automatically register the tumor in the end-expiration phase to the tumor in the end-inspiration phase. Non-synchronous marker motion was defined by the vector connecting a marker on the end-expiration phase CT-scan to the corresponding marker on the registered end-inspiration phase CT-scan. The tracking error was defined as the difference in the center of mass of the included markers on the end-expiration CT-scan and the registered end-inspiration CT-scan. Multivariate linear regression analysis was performed to evaluate the association between non-synchronous marker motion and 1) the amplitude of tumor motion, 2) the distance between the marker and the tumor edge, 3) the location of the marker relative to the tumor (same lobe or different lobe) 4) the type of marker (coil or percutaneously-placed marker) and 5) the location of the tumor (against the chest wall or not). We examined if the tracking error could be reduced by excluding markers for tumor tracking based on 1) the distance of the marker to the tumor edge and 2) the extent of non-synchronous marker motion during breathing as determined on the 4DCT scan. The value of the two exclusion parameters was varied such that for all patients at least 1 marker was available for tracking.
Results: Non-synchronous marker motion during the breathing cycle was 0.2±1.4 mm (mean±1SD) in LR direction, 0.4±1.6 mm in AP direction, and -0.3±2.9 mm in CC direction. Factors which significantly increased non-synchronous motion were increasing amplitude of tumor motion ($p<0.01$), increasing distance between the marker and the tumor edge ($p<0.01$), and the location of the tumor against the chest wall ($p<0.01$). The tracking error due to non-synchronous tumor marker motion could be reduced by excluding markers based on the distance of the marker to the tumor edge (fig 1a). More effective was excluding markers based on their non-synchronous motion during breathing as assessed by 4DCT. By excluding markers with non-synchronous motion ≥3.5 mm, the standard deviation of the tracking error was reduced from 1.4 to 0.8 mm (LR), 1.2 to 1.0 mm (AP), 2.0 to 0.9 mm (CC) (fig 1b).

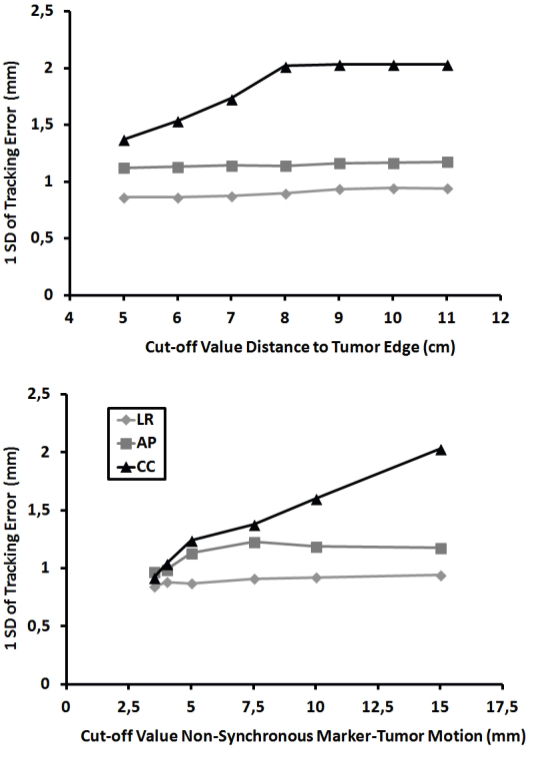

Conclusions: Precise tumor tracking requires a 4DCT scan to identify and exclude markers with non-synchronous motion. This allows a reduction in the standard deviation of the tracking error by as much as 50%. Exclusion of markers based on the distance to the tumor edge was less effective.

OC-0334
Actively triggered cone-beam CT acquisition based on electromagnetic respiratory motion tracking
M.F. Fast[1], U. Oelfke[1], S. Nill[1]
[1]*German Cancer Research Center (DKFZ), Academic Physics, Heidelberg, Germany*

Purpose/Objective: 4D CBCT images acquired on linac-based scanners are usually reconstructed by extracting the motion information from the 2D projections (or an external surrogate signal), and binning the individual projections into one or multiple breathing phases. In this 'after-the-fact' binning approach, however, imaging dose might be administered in breathing phases not desired for reconstruction. For 4D reconstructions, the image quality can be compromised by an uneven distribution of projections over respiratory phases and angles. We have therefore developed control software which actively triggers 2D projections based on the predicted position of the tumour. The prediction is derived from internal tumour positions reported by the Calypso electromagnetic (EM) tracking system.
Materials and Methods: Due to the radio emissions of the EM-array, it is impossible to simultaneously operate EM tracking and acquire artefact-free images without shielding the detector. For this study we have used a very thin aluminium Faraday 'cage' for the detector that removes most EM-induced artefacts. We have also implemented new control software which receives a continuous stream (10 Hz) of 3D tumour positions from the EM-device. The position information of a sliding training window is used to predict a new position (120 ms in the future) using a support vector machine. The predicted position is then classified as e.g. peak-inhale according to the amplitude of the last respiratory cycle. Depending on the desired breathing phase and maximum angular spacing between images, a new 2D projection is triggered. We have used a lung phantom moving on a $\sin^4$ trajectory with 15 mm amplitude and a 3.5 sec period for our study. A tumour model made from RW3 and the EM transponders were implanted into the phantom. For kV images which were superimposed by the projection of the EM-array (i.e. its internal antenna), image processing was used to replace pixels depicting the antenna by neighbouring 'good' pixels. 3D images were then reconstructed using an FDK algorithm provided by Siemens.